



NRC Publications Archive Archives des publications du CNRC

Tailoring the surface of a gene delivery vector with carboxymethylated dextran: a systematic analysis

Fortier, Charles; Louvier, Elodie; Durocher, Yves; De Crescenzo, Gregory

This publication could be one of several versions: author's original, accepted manuscript or the publisher's version. / La version de cette publication peut être l'une des suivantes : la version prépublication de l'auteur, la version acceptée du manuscrit ou la version de l'éditeur.

For the publisher's version, please access the DOI link below. / Pour consulter la version de l'éditeur, utilisez le lien DOI ci-dessous.

Publisher's version / Version de l'éditeur:

<https://doi.org/10.1021/acs.biomac.5b00221>

Biomacromolecules, 16, 6, pp. 1671-1681, 2015-04-15

NRC Publications Record / Notice d'Archives des publications de CNRC:

<https://nrc-publications.canada.ca/eng/view/object/?id=ab1c9b68-9dc8-474c-a7ca-0ed13201ac54>

<https://publications-cnrc.canada.ca/fra/voir/objet/?id=ab1c9b68-9dc8-474c-a7ca-0ed13201ac54>

Access and use of this website and the material on it are subject to the Terms and Conditions set forth at

<https://nrc-publications.canada.ca/eng/copyright>

READ THESE TERMS AND CONDITIONS CAREFULLY BEFORE USING THIS WEBSITE.

L'accès à ce site Web et l'utilisation de son contenu sont assujettis aux conditions présentées dans le site

<https://publications-cnrc.canada.ca/fra/droits>

LISEZ CES CONDITIONS ATTENTIVEMENT AVANT D'UTILISER CE SITE WEB.

Questions? Contact the NRC Publications Archive team at

PublicationsArchive-ArchivesPublications@nrc-cnrc.gc.ca. If you wish to email the authors directly, please see the first page of the publication for their contact information.

Vous avez des questions? Nous pouvons vous aider. Pour communiquer directement avec un auteur, consultez la première page de la revue dans laquelle son article a été publié afin de trouver ses coordonnées. Si vous n'arrivez pas à les repérer, communiquez avec nous à PublicationsArchive-ArchivesPublications@nrc-cnrc.gc.ca.



Tailoring the Surface of a Gene Delivery Vector with Carboxymethylated Dextran: A Systematic Analysis

Charles Fortier,^{†,‡} Elodie Louvier,^{‡,§} Yves Durocher,^{‡,§} and Gregory De Crescenzo^{*,†}

[†]Department of Chemical Engineering, Groupe de Recherche en Sciences et Technologies Biomédicales (GRSTB), École Polytechnique de Montréal, P.O. Box 6079, succ. Centre-Ville, Montreal (QC), Canada H3C 3A7

[‡]Life Sciences | NRC Human Health Therapeutics Portfolio, Building Montreal-Royalmount, National Research Council Canada, Montreal (QC), Canada H4P 2R2

[§]Département de Biochimie et Médecine Moléculaire, Université de Montréal, Montréal (QC), Canada H3C 3J7

S Supporting Information

ABSTRACT: Polymeric nanocarriers are attractive nonviral vectors for gene delivery purposes *in vivo*. For such applications, numerous physiological and subcellular bottlenecks have to be overcome. In that endeavor, each structural feature of nanocarriers can be optimized with respect to its corresponding challenges. Here, we focused on the interface between a model gene delivery nanocarrier and relevant constituents of the physiological environment. We screened a library of carboxymethylated dextrans (CMD) for the electrostatic coating of positively charged nanocarriers. We evaluated the joint influence of the CMD molecular weight and charge density upon nanocarrier coating with respect to DNase, small ions, plasma proteins, red blood cells, and target cells. A total of 4 out of 26 CMD coated nanocarriers successfully passed every screening assay, but did not yield increased reporter gene expression in target cells compared to uncoated nanocarriers. The fine-tuning of CMD for nanocarrier coating yielded a relevant shortlist of candidates that will be further tested *in vivo*.



INTRODUCTION

There is a growing body of evidence toward the feasibility of polymeric nanocarrier-based cancer gene therapy.^{1,2} Mainly used as nucleic acid condensing agents, polymers have also been employed as coating materials³ in an effort to decouple the biointerface and the core of nucleic acid nanocarriers.⁴ The results of several studies on the charge density of cationic polymers, as core constituents of nanocarriers, have been reported.⁵ Yet, systematic analyses of other polymers of interest and, particularly, polyanions for the surface modification of nanocarriers are scarce.^{4,6–9} Such systematic analyses *in vitro* should feature relevant assays that bear predictive power with respect to nanocarrier performance *in vivo*.^{2,10}

Anionic polymers, particularly, polysaccharides, have been tested as surface modifiers for nanocarrier-based gene delivery purposes.^{11,12} Significant advances have been reported in terms of systemic residence, cytotoxicity, biodegradability, and cell targeting,¹³ which were generally attributed to the nature of the polysaccharides rather than to their structure. Regarding the latter, molecular weight has already been optimized in several studies,^{7–9} but coupled fundamental properties of these polyanions such as molecular weight and charge density have yet to be concomitantly optimized. We sought to carry out a systematic analysis on those parameters in order to aid the design of future nanocarriers. We based our approach on dextran, a well-characterized neutral biopolymer.

Dextran and its derivatives have found relevant applications in biomedical engineering and healthcare. For instance, aqueous solutions of dextran featuring high oncotic pressure, low antigenicity, low thrombogenicity, and low erythrocyte aggregation have been used as blood volume expanders to treat moderate blood loss.¹⁴ Carboxymethylated dextran (CMD) has been reported to feature additional relevant properties, such as higher systemic residence half-life compared to dextran,¹⁵ favorable uptake by tumor cells,¹⁶ and the ability to electrostatically coat positively charged nanoparticles.¹⁶ Dextran and CMD being highly hydrophilic, flexible, and easy to functionalize, these polymers have also been employed as low-fouling versatile coatings that limit nonspecific adsorption at the surface of surface plasmon resonance (SPR)-based biosensor chips¹⁴ and multiple-well plates for enzyme-linked immunosorbent assays (ELISA).¹⁷ Taken together, those properties make the CMD polymer family an interesting candidate for nanoparticle coating in the context of nucleic acid delivery for gene therapy.

The interactions of dextran- and CMD-coated nanoparticles with human cells have already been studied *in vitro* and *in vivo* with magnetic nanoparticles.^{16,18–20} These reports form an

Received: February 16, 2015

Revised: April 10, 2015

Published: April 15, 2015

encouraging picture regarding the use of CMD as a surface modifier in terms of cytocompatibility and cellular uptake. In particular, although no known cell receptor has been associated with the uptake of dextran by cells,¹⁸ CMD-coated nanoparticles exhibited a degree of cell selectivity toward tumor cells in uptake studies.¹⁶ The authors conjectured that the distinctive α -1 \rightarrow 6 glycosidic linkage of dextran was involved in that latter point. In the field of gene therapy, only a few reports can be found on the use of either dextran or CMD for nucleic acid delivery, a majority of which dealing with polymer conjugates^{12,21–23} rather than with nanoparticle coating.²⁴ Besides, results and discussions from these studies were mostly focused on a single polymer formulation of given molecular weight and charge density.^{22–24} Thus, CMDs arguably appear to be relevant biomaterials in the context of the surface modification of nanoparticles in various cancer therapies.

Here we carried out a systematic analysis on the use of CMD for the coating of a model nanocarrier. More precisely, we postulated that the molecular weight and the degree of carboxymethylation of the polymer were two parameters worth optimizing for the electrostatic coating of positively charged nanoparticles with CMD. We thus tested a CMD library encompassing a large spectrum of molecular weights and charge densities. As a model gene delivery nanoparticle, we chose branched polyethylenimine (bPEI)/plasmid DNA (pDNA) complexes, referred here as polyplexes, that are known to feature high transfection capabilities *in vitro*, but poor *in vivo* outcomes.²⁵ Schematically, on the one hand, bPEI, a strongly positive polyelectrolyte, is able to condense pDNA and to buffer the endosomes so as to escape lysosomal degradation.²⁶ On the other hand, bPEI exhibits a dose-dependent cytotoxicity, especially in its free form, and it has been reported to cause harmful host responses, including erythrocyte aggregation, cytopenia, and capillary clotting *in vivo*.^{25,27} As such, bPEI/pDNA polyplexes represent a valid core nanoparticle to coat with CMD. We chose an amine of bPEI-to-phosphate of pDNA (N/P) ratio of 6:1 to prepare core polyplexes, as that formulation has often been used with this polymer.^{28,29}

After determining the appropriate amounts of CMD to be added to warrant colloidal stability of our polyplexes, the jointed impact of charge density and chain length of our CMD upon polyplex stability, DNA protection to nuclease, plasma protein adsorption and erythrocyte aggregation were investigated. At last, to implement our *in vitro* cell-based assays, we chose the human cancer-derived epidermal growth factor receptors (EGFR)-bearing A549 cells. This cell line with moderately overexpressed EGFR has already been used as a model target in cancer research.^{30,31} Besides, using this cell line allowed us to perform a proof-of-concept biofunctionalization of CMD to target EGFR.

MATERIALS AND METHODS

Chemical Reagents and Biomolecules. Divinyl sulfone (DVS, 99.7% purity), tris(2-carboxyethyl)phosphine (TCEP) hydrochloride solution (0.5 M), HEPES (99.5+% purity), monobromoacetic acid (99+% purity), 2-mercaptoethanol (99+% purity), branched PEI 25 kDa (99+% purity), Hoechst 33342 (98+% purity), DNase I (type IV from bovine pancreas), heparin (sodium salt, grade 1-A), and human plasma (pooled, in 3.8% trisodium citrate) were purchased from Sigma-Aldrich Canada, Ltd. (Oakville, ON). All dextrans (technical grade T) were purchased from Pharmacosmos A/S (Holbaek, Denmark). Deuterium oxide (99% purity) was purchased from Cambridge Isotope Laboratories, Inc. (Andover, MA). DMEM,

YOYO-1 iodide (1 mM solution in DMSO), and SYBR Safe (10000 \times in DMSO) were purchased from Invitrogen Corp. (Burlington, ON). HyClone Cosmic fetal calf serum (FCS) was obtained from Thermo Scientific, Ltd. (Pittsburgh, PA). Accutase (in Dulbecco's PBS containing 0.5 mM EDTA) was obtained from Innovative Cell Technologies, Inc. (San Diego, CA). Cysteine-tagged Kcoil peptides were synthesized by the peptide facility at the University of Colorado (Denver, CO) and aliquoted in acetic acid (0.1% v/v) upon reception. Ecoil-tagged EGF (Ecoil-EGF) was produced in HEK293–6E cells and was purified by immobilized metal-ion chromatography as previously described.³² The purified protein was then desalted, quantified by absorbance at 280 nm on a Nanodrop ND-1000 (Thermo Scientific) before being sterile-filtered, aliquoted, and stored at -80 °C until use. Quantification was confirmed by ELISA with the Human EGF DuoSet from R&D Systems (Minneapolis, MN), and purity was evaluated by SDS-PAGE.

Preparation and Characterization of Carboxymethylated Dextrans and Conjugates. The carboxymethylation of dextrans was adapted from a previously described protocol.¹⁷ CMD obtained from the same technical grade dextran were prepared from a common batch reaction whereby fractions were quenched at different times. For example, dextran T70 (65 kDa, 800 mg) was dissolved in ultrapure water (13 mL) with NaOH (5 M). The reaction was initiated by adding monobromoacetic acid (9 mL, 2 M) to the reaction mixture. The reaction was carried out at room temperature under constant stirring. Fractions (2.75 mL) were quenched with HCl (0.45 mL, 14.1 M) at eight different times starting from 2.65 min up until 120 min. The nomenclature of CMD corresponds to the rounded molecular weight in kDa and carboxymethylation time in min (e.g., CMD70–30). Each fraction was subsequently desalted by five consecutive centrifugal filtrations in ultrapure water using Amicon Ultra-15 devices with a cutoff of 10 kDa before freeze-drying.

The degree of carboxymethylation of each CMD was evaluated by ^1H NMR. Samples from each polymer were dissolved in deuterium oxide (5 g/L) to be evaluated on a Varian Unity Inova 400 MHz instrument (Agilent Technologies, Inc., Mississauga, ON). Samples were probed at 50 °C, and the H_2O signal was pulsed out of the spectra. Chemical shifts were derived relatively to tetramethylsilane.

For the preparation of Kcoil-peptide-conjugated CMD (CMD70–30-Kcoil), CMD70–30 was first modified with divinyl sulfone by adapting the method described by Yu et al.³³ Briefly, CMD70–30 powder was dissolved in ultrapure water (0.34 M of hydroxyl groups) with NaOH (0.1 M). Then, pure DVS was quickly added (0.43 M). After 3 min, HCl (5 M) was added to decrease the pH down to 5. The resulting CMD70–30-VS intermediate was then purified by five consecutive centrifugal filtrations in ultrapure water using an Amicon Ultra-15 device with a cutoff of 10 kDa. Subsequently, CMD70–30-VS (2.5 μM of macromolecules) was diluted in PBS (10 mM, pH 7.4) with TCEP (5 mM) and Kcoil³⁴ (14.34 μM). The reaction mixture was agitated in the dark for 2 days and ultimately quenched with 2-mercaptoethanol (50 mM). The final CMD70–30-Kcoil was similarly purified with a 10-kDa cutoff Amicon Ultra-15 device. The Kcoil/CMD ratio was evaluated to be about 4.9:1 by size exclusion chromatography (see Supporting Information, Figure 6).

Preparation of Polyplexes. All solutions were prepared at room temperature in water buffered with HEPES (10 mM, pH 7.4), referred to as the complexation buffer. To form polyplexes, one volume of bPEI was added to one volume of pDNA solution (40 $\mu\text{g}/\text{mL}$ of pTT-BFPq plasmid coding for the blue fluorescent protein BFP)³⁵ to reach an N/P ratio of 6:1. The resulting suspension was immediately vortexed and was further incubated for 5 min to form core polyplexes. Subsequently, one volume of CMD was added, and the resulting mix was immediately vortexed and further incubated for 30 min to reach a C/N/P ratio of 3:6:1, unless otherwise specified. For Kcoil-containing polyplexes, a mix of CMD and CMD-Kcoil was used at that step in order to adjust the Kcoil concentration. Finally, one volume of Ecoil-EGF (0.68 μM) was added, and the final suspension was immediately vortexed and further incubated for 5 min to form targeted coated polyplexes.

Agarose Gel Electrophoresis. For gel shift assays focused on polyplex cohesion, samples (130 ng of pDNA) were loaded in each well in a 1% w/v agarose Tris-acetate EDTA buffer gel stained with SYBR Safe (1×). Electrophoresis was carried for 30 min at 120 V and 400 mA. Gels were imaged with a ChemiDoc MP System (Bio-Rad Ltd., Mississauga, ON). Quantitative band fluorescence analyses were carried out with Image Lab 5.0 and ImageJ.

For polyplex challenging with DNase I, we adapted a previously reported method.³⁶ Briefly, polyplexes were prepared as described above and were then incubated with DNase I (0.2 Kunitz unit/μg of DNA) at 37 °C for 30 min, after which DNase I activity was stopped by the addition of EDTA (5 mM). Polyplexes were then dissociated by a 30 min incubation with heparin (5 mg/mL) at 37 °C. Finally, samples (50 ng of pDNA) were loaded on agarose gels and were processed as mentioned above.

Dynamic Light Scattering. Dynamic light scattering (DLS) for hydrodynamic diameter and zeta potential measurements were performed on a ZetaSizer Nano ZS (Malvern Instruments, Ltd.) in manual mode with the Zetasizer software in order to monitor the kinetics of salt-induced aggregation. The following sequence was used: a core polyplex suspension was formed and was then probed thrice for hydrodynamic diameter by six runs of 6 s each; then CMD was added as described earlier. The suspension was then split in two for subsequent size and zeta potential measurements, as the latter measurement may tamper with the sample. The coated polyplexes were similarly probed thrice before the addition of an appropriate volume of concentrated PBS (3×) to raise the salt concentration up to physiological level. The hydrodynamic diameter of each formulation was then probed every 15 s for 15 min (3 runs of 3 s each) to evaluate aggregation kinetics; and the initial slope in nanometers per min was extracted from the data.

Scanning Electron Microscopy. Polyplex suspensions were sprayed on a silicon wafer substrate that was then air-dried. After gold sputter-coating with an Agar Manual Sputter Coater (Marivac, Inc., Gore, QC), nanoparticles were imaged in high vacuum mode at 20 kV on a Quanta 200 FEG environmental scanning electron microscope (SEM; FEI Company, Hillsboro, OR).

Adsorption of Plasma Proteins on Polyplexes. Polyplex suspensions were prepared as described above. Each one was then incubated with human plasma (2% v/v) for 30 min at 37 °C, after which samples were centrifuged at 20000 × g for 30 min to pellet the polyplexes. The supernatant was carefully removed, and the pellet was rinsed once with complexation buffer. Whole pellets (1.3 μg of pDNA) were then dissociated in 1× nonreductive SDS-PAGE loading buffer for 10 min at 70 °C and were finally processed by SDS-PAGE with Coomassie staining.

Erythrocyte Aggregation Assay. Erythrocytes from sheep (50% suspension in alsevers, Rockland, Inc., Gilbertsville, PA) were washed three times in PBS by centrifugation at 400 × g for 10 min and were then diluted 5-fold in PBS. Polyplexes were prepared in 1× PBS, as described above for DLS experiments. Immediately after addition of PBS to the preformed polyplexes, erythrocytes were further diluted 10-fold with polyplexes in 48-well plates (final volume of 250 μL per well). After a 30 min incubation at 37 °C under 120 rpm shaking, 3270 μm × 360 μm phase images were randomly taken from each well with an AX10 microscope (Zeiss, Peabody, MA). A microscopic aggregation index (MAI, corresponding to the fraction of the surface covered with erythrocytes) was derived from an automated particle analysis performed with ImageJ.

Cell Culture. A549 cells were maintained in DMEM supplemented with 10% FCS, further referred to as complete medium. Cultures were kept at 37 °C in a humidified, 5%-enriched CO₂ and water-jacketed incubator. For passages and seedings, Accutase was used to gently detach cells. A given culture was maintained for no more than 15 passages until another cell aliquot was thawed.

Transfection. A total of 18 h before transfection, A549 cells were distributed in 24-well plates (0.5 mL, ca. 80000 cells per mL) to let them settle on the culture plate surface and reach about 80% of confluence at the time of transfection. For each well, the medium was discarded just before adding the polyplex suspension diluted 10-fold in

fresh complete medium that was quickly vortexed. After 4 h post-transfection (hpt), suspensions were discarded and wells were rinsed with PBS. Fresh complete medium containing free bPEI to a virtual N/P ratio of 24:1 was ultimately added.

Flow Cytometry. To study the uptake of polyplexes, pDNA was stained with YOYO-1 at a ratio of 1 dye molecule per 50 base pairs. Two days post-transfection (dpt), cells were treated with Accutase. Aggregates from each sample were removed by filtration through a 310-μm Nitex mesh mounted on a 1 mL syringe. Flow cytometry was performed on an LSR II (Becton-Dickinson and Co., Franklin Lakes, NJ). A total of 10000 live cells (from events gated in a side scatter vs forward scatter dot plot) were gated to count YOYO-1-positive cells as well as BFP-positive cells on the FACSDiva software.

Confocal Microscopy. Detached cells (2 mL, 80000 cells per mL) were seeded on 35 mm glass bottom dishes (MatTek Corp., Ashland, MA). A total of 5 min before transfection, cells were stained with Hœchst 33342 (5 μM) in complete medium at 37 °C. Images were captured 10 min post-transfection (mpt) and 4 hpt using an FV10i-DOC confocal microscope (Olympus Corp., Tokyo, Japan) with a 1.35 NA 60× oil-immersed objective. Live cells were imaged in an INUBG2E-FV10i 5%-enriched CO₂ water-jacketed incubator stage (Tokai Hit CO., Ltd., Fujinomiya, Japan).

Statistical Analysis. Statistical significance annotations are the result of unpaired two-tailed Student's *t*-test; * indicates *p* < 0.05; ** indicates *p* < 0.01; and # indicates no significant difference at 5%.

RESULTS AND DISCUSSION

Synthesis of the CMD Library. To quantify precisely the degree of carboxymethylation (*dcm*) of our CMDs, each of them was first characterized by ¹H NMR spectroscopy. We took advantage of the signal yielded by the hydrogen borne by the anomeric carbon C1 of the anhydroglucose unit (see Figure 1) to derive the *dcm* at position C2. We then derived the total *dcm* (on either positions C2, C3, or C4) by taking into account the known relative proportions of carboxymethylation on those sites in our reaction conditions, namely, C2/C3/C4 12:5:8.³⁷ The *dcm* and the mass (including the mass increase resulting

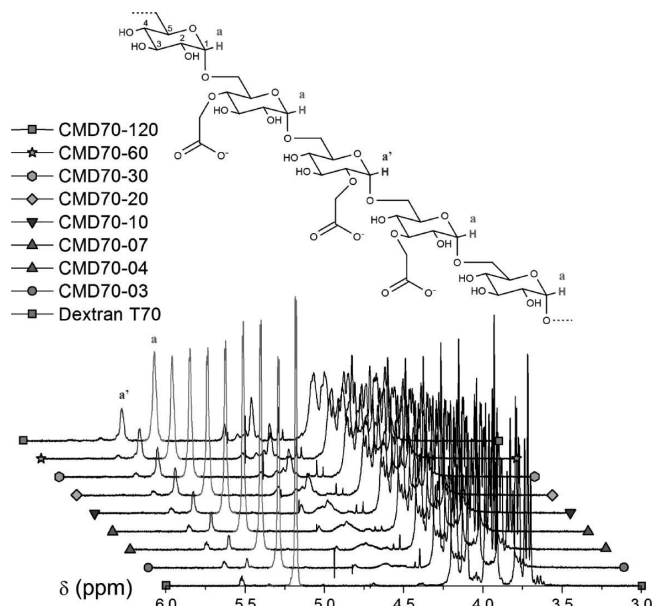


Figure 1. Schematic molecular structure of CMD (top) and ¹H NMR spectra of the 70 kDa CMD series (bottom). Anomeric hydrogen atoms corresponding to pristine or modified anhydroglucose units (a and a') are highlighted and associated with their corresponding peaks in the given spectra. The nomenclature of our dextran derivatives is described in Table 1.

from the addition of the carboxymethyl moieties), as well as the charge density (expressed in negative charge per kDa, \ominus /kDa) for the 26 CMDs forming our library are listed in Table 1.

Formulation of CMD/bPEI/pDNA-Coated Polyplexes.

Core polyplexes resulting from the complexation of bPEI and pDNA were obtained using a N/P ratio of 6:1. Upon formation, core polyplexes remained stable for at least an hour in complexation buffer (HEPES, 10 mM, pH 7.4; data not shown), in good agreement with other reports.^{26,38} Then, we incubated core polyplexes with CMD for at least 30 min in order to let the ternary mix reach equilibrium. By adding CMD to bPEI/pDNA polyplexes, our rationale was to coat preformed core polyplexes as well as to complex residual free bPEI in the suspension.

We first evaluated the impact of incubating core polyplexes with increasing amounts of CMD upon the size of the resulting ternary polyplex by measuring the average hydrodynamic diameter and zeta potential for each nanoparticle suspension. The carboxylate-to-amine-to-phosphate or C/N/P ratio was used to describe each formulation. We hypothesized that a minimal amount of CMD would be required to decorate the bPEI/DNA polyplexes while complexing all free bPEI (thus preventing the latter from promoting the aggregation of CMD-coated nanoparticles). The data collected for representative CMDs from our library are reported on Figure 2. As expected, when core polyplexes were incubated with CMD at a C/N/P ratio of 0.5:6:1 or 1:6:1, polyplexes with a positive zeta potential were observed (Figure 2B). When incubated with higher amounts of CMD (C/N/P of 3:6:1 and higher ratios), newly decorated polyplexes remained stable, with no measurable change in hydrodynamic diameter (Figure 2A) and with a recharged zeta potential plateauing at a range of negative values (Figure 2B).

We previously reported that, for a N/P ratio of 6:1, bPEI/pDNA polyplexes accounted for about N/P 2.5:1 out of a total of 25 kDa bPEI, with the remaining about N/P 3.5:1 excess polycation being in free form;³⁹ in good agreement with the literature.^{27,40} Here, we observed that at a C/N/P ratio between 1:6:1 and 1.5:6:1, zeta potential reversal occurred, along with strong aggregation in complexation medium. The acidity range of the carboxymethyl moieties of CMD indicates that carboxylate is the preponderant form at physiological pH.⁴¹ Conversely, the N/P ratio of the core polyplex formulation (2.5:1) suggests that roughly 1 in every 2.5 amino groups in bPEI is protonated when complexed with a polyelectrolyte at pH 7.4, if we assume that almost all the positive charges of a given bPEI chain can interact with the negative charges displayed by pDNA. That led us to conclude that for the remaining free bPEI in solution (corresponding to N:P 3.5:1 out of 6:1), only about 1.4 out of 3.5 would be protonated when complexed with excess CMD, in good agreement with the observed threshold C/N/P ratio between 1:6:1 and 1.5:6:1 in coated polyplex formulation (Figure 2A,B). For the rest of the study, we chose to work at a C/N/P ratio of 3:6:1, which consistently yielded polyplexes in the 100 nm range.

In an effort to best characterize our formulations, we also conducted titrations of bPEI alone by CMD70–30, which yielded to the formation of ghost polyplexes in the 100 nm hydrodynamic diameter range (see Supporting Information, Figure 1). Our DLS results indicated that a C/N ratio of about 0.4:1 corresponded to charge equivalence, as suggested by both a strong aggregation (Supporting Information, Figure 1A) and an annulled zeta potential (Supporting Information, Figure 1B)

Table 1. Characteristics of the 26 Polymers Forming our CMD Library^a

precursor	dextran T10										dextran T40									
	CMD10–10	CMD10–20	CMD10–30	CMD10–60	CMD10–120	CMD40–02	CMD40–03	CMD40–05	CMD40–10	CMD40–20	CMD40–30	CMD40–60	CMD40–120	CMD70–10	CMD70–20	CMD70–30	CMD70–60	CMD70–120		
<i>d_{hm}</i> (%)	17.4	25.9	33.0	44.5	73.2	3.9	6.2	8.8	16.4	27.2	34.8	45.2	57.9	19.4	30.5	35.0	47.4	56.3		
charge density (\ominus /kDa)	1.01	1.46	1.82	2.37	3.58	0.24	0.37	0.53	0.96	1.53	1.91	2.40	2.96	1.12	1.70	1.92	2.50	2.89		
molecular wt (kDa)	10.5	10.8	11.1	11.5	12.5	39.0	39.4	39.7	40.8	42.2	43.3	44.7	46.5	23.0	23.8	24.2	25.1	25.8		
precursor	dextran T70										dextran T70									
<i>d_{hm}</i> (%)	19.4	30.5	35.0	47.4	56.3	7.6	11.7	16.8	23.7	32.8	39.4	48.6	56.9	19.4	30.5	35.0	47.4	56.3		
charge density (\ominus /kDa)	1.12	1.70	1.92	2.50	2.89	0.46	0.70	0.98	1.35	1.81	2.13	2.56	2.92	1.12	1.70	1.92	2.50	2.89		
molecular wt (kDa)	23.0	23.8	24.2	25.1	25.8	66.8	67.7	68.9	70.5	72.6	74.2	76.3	78.2	23.0	23.8	24.2	25.1	25.8		

^aNote that the name of each CMD indicates the size of the dextran used (first number, in kDa) and the duration of the carboxymethylation reaction (second number, in min).

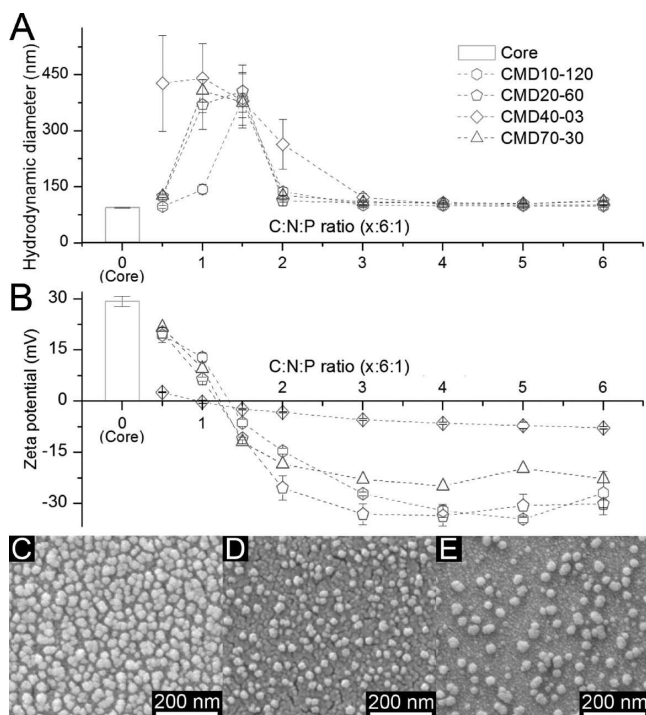


Figure 2. Dependence of the size (A) and charge (B) of polyplexes on the C/N/P ratio; representative scanning electron micrographs (SEM) of polyplexes at the C/N/P 3:6:1 ratio (C–E). For dynamic light scattering (DLS) measurements, core polyplexes at an N/P ratio of 6:1 were incubated with varying amounts of either CMD10–120, CMD20–60, CMD40–03, or CMD70–30. The zeta potential and the hydrodynamic diameter were measured in complexation buffer. SEM micrographs illustrate core polyplexes at a N/P ratio of 6:1 (C), polyplexes coated with CMD70–30 at a C/N/P ratio of 3:6:1 (D), and ghost polyplexes made of bPEI and CMD70–30 at a C/N ratio of 3:3.5 (E).

of these polyplexes. Those observations unambiguously validated the protonation degree of bPEI we postulated (see above) and the nanoparticulate nature of ghost polyplexes that were also observed by scanning electron micrograph (SEM; Figure 2E). SEM and DLS measurements were not in agreement for the size of the particles. SEM observations may lead to an underestimation of the size of these nanoparticles, as samples had to be dehydrated and adsorbed on a substrate for imaging.⁴² Conversely, the hydrodynamic diameter deduced from DLS measurements might have been overestimated for several reasons: first, the assumption that the shape of our polyplexes was spherical does not hold true (Figure 2C–E); second, a subpopulation of oligomerized nanoparticles might have resulted in an overestimation of the intensity-weighted hydrodynamic diameter, as larger particles scatter more light than smaller ones.⁴⁰

Encapsulation and Protection of pDNA. Once the physical relevance of coating bPEI/pDNA polyplexes with CMD was asserted, we carried out a biophysical characterization of coated polyplexes generated from our CMD library. First, the question whether CMD displaced pDNA from polyplexes was addressed by gel shift assays (Figure 3). It appeared that an increase in charge density and to a lesser extent in molecular weight caused pDNA to migrate in the agarose gel in the form of a smear. Those results suggest that CMD can compete with pDNA if the charge density of the former is high enough (see Supporting Information, Figure

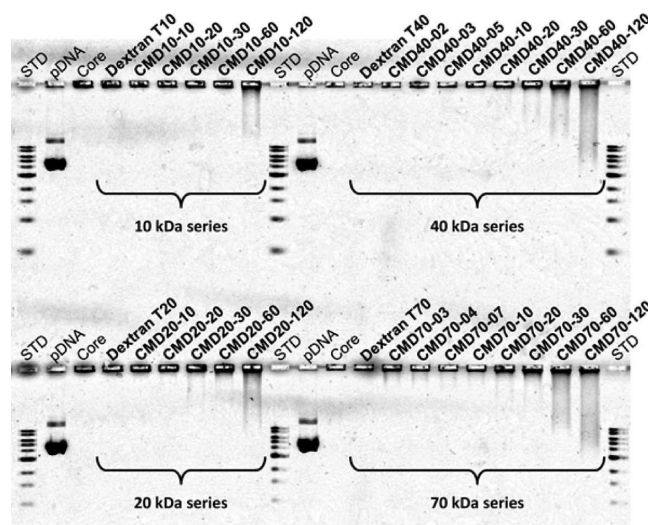


Figure 3. Influence of CMD on encapsulated pDNA release from polyplexes. Representative electrophoretic patterns of coated polyplexes and controls on agarose gel.

2A), that is, close or higher than the charge density of DNA: about $3 \ominus/\text{kDa}$. We assumed that there exists a threshold for the charge density of the polyplex-coating polyanion beyond which resulting assemblies are no longer fit for *in vivo* gene delivery. For instance, heparin, that we used to dissociate our polyplexes, has a charge density that is beyond that threshold. We estimated that CMD40–120 and CMD70–120 also crossed that threshold, as both caused more than 10% of total pDNA to smear out of the wells in the agarose gels (see Figure 4 and Supporting Information, Figure 2A).

Then, in order to test whether pDNA was still protected against nucleolytic degradation upon coating of polyplexes with CMD, we challenged our polyplex suspensions with DNase I. We then analyzed the profile of the pDNA cargo in agarose gel electrophoresis (Figure 4). When unchallenged control core

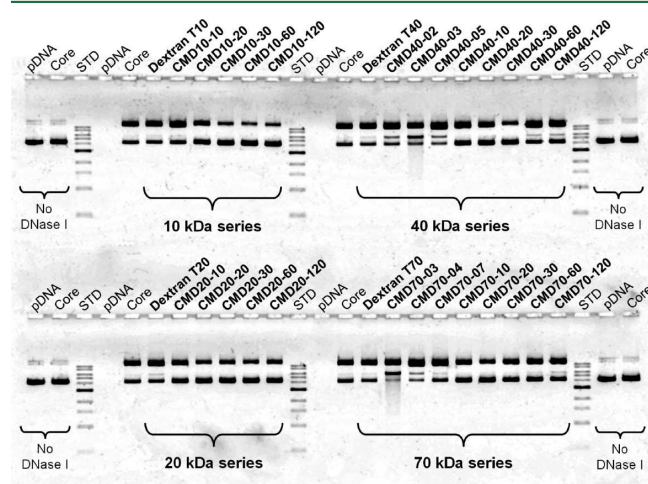


Figure 4. Influence of CMD on the ability of polyplexes to protect pDNA against DNase I. Representative electrophoretic patterns of coated polyplexes and controls after DNase I challenging followed by polyplex dissociation. Naked pDNA controls challenged by DNase I were completely degraded. Controls that were not challenged by DNase I are presented on the two first and the two last wells of each front of the agarose gel.

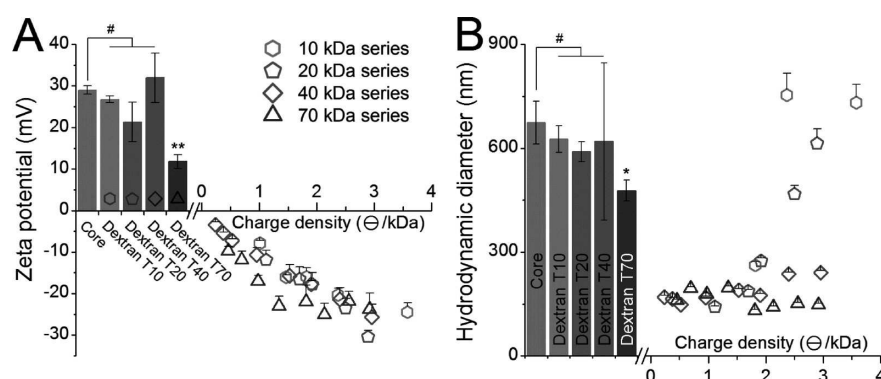


Figure 5. Influence of the charge density of CMD on the colloidal properties of polyplexes. The zeta potential (A) was collected by DLS on fresh polyplexes after 30 min in complexation buffer. The hydrodynamic diameter (B) was averaged from data collected from 10 to 15 min after the addition of PBS. Bars represent control core polyplexes alone or in the presence of pristine dextran. Note that no measurement was possible for CMD10–10 and CMD10–20, for coated polyplexes aggregated in complexation buffer even before the addition of PBS; # not significantly different at 5% from core formulation; * and ** significantly different from core formulation ($p < 0.05$ and $p < 0.01$, respectively).

polyplexes were subjected to dissociation with heparin, they revealed a strong predominance of the supercoiled form, similarly to the unchallenged naked pDNA control. For every polyplex formulation that was challenged with DNase I, the fraction in relaxed form increased. It seems thus reasonable to assume that the experimental conditions for the challenging with DNase I caused that increase, regardless of the polyplex formulation.

Surprisingly, results indicated a significant degradation of pDNA from polyplexes coated with CMD40–03 and with CMD70–03, whereby a smear of low molecular weight DNA fragments appeared on the gel. That smear was accompanied by a brighter band identified as linearized pDNA for those two formulations and their neighboring ones. As that sensitive spot seemed to correlate with a narrow charge density range, we pooled additional CMDs from different batches in order to study that effect in greater detail. Results summarized in Supporting Information, Figure 3 indicate that CMDs with a charge density between 0.3 and 0.4 Θ/kDa failed to protect pDNA from DNase I in the conditions of our tests. That range corresponds to one carboxymethyl on every 20 to 15 anhydroglucose units along the backbone of CMD. Those puzzling observations warrant further investigation on the interactions located at the polyplex interface.

Apart from that narrow charge density range, a slight correlation was found between pDNA displacement by CMD (smear pDNA on Figure 3) and pDNA protection against DNase I (degraded pDNA on Figure 4; see Supporting Information, Figure 2B). This correlation probably indicates that the pDNA displaced by CMD was degraded by DNase I, but the encapsulated pDNA was well protected. Still, the dissimilarities between the overall results of those two tests based on agarose gel electrophoresis clearly show that they probe distinct polyplex features. Our results thus highlight both assays should be carried out when characterizing a gene delivery vector. It is also of interest to note that we used 0.2 Kunitz unit of DNase I per microgram of pDNA for our challenging assays. We hypothesized that such conditions *in vitro* did not reflect the actual nuclease activity encountered by polyplexes during transfection. Therefore, it seemed reasonable to assume that about 30% degradation of cargo pDNA in these challenging conditions did not correlate with as much degradation of pDNA throughout the transfection process. Rather, we believe that such a stringent test allowed us to estimate the stability of

polyplexes. By gaining insight into the entrapment tightness of cargo pDNA, we could then anticipate the appropriate release of the latter during transfection.

Size, Charge, and Aggregation Trends. We then characterized the various polyplexes we generated by DLS. The zeta potential of freshly formed polyplexes was measured in complexation buffer (Figure 5A). For the first three CMD series, we observed that the zeta potential of coated polyplexes was strongly correlated to the charge density of the CMD but not to their molecular weight. Unexpectedly, the dextran T70 caused a significant decrease in zeta potential. That influence of a longer polymer chain translated into a markedly stronger charge reversal of polyplexes coated with CMDs of the 70 kDa series, until the zeta potential plateaued to about -24 mV at 1.35 Θ/kDa .

The size distribution was monitored after adding salt at a physiological concentration (Figure 5B). For all formulations, the polydispersity index (PDI) remained within 0.1 and 0.3 (data not shown). Such PDI values are expected when dealing with slightly heterogeneous populations comprising plasmid-containing polyplexes and ghost polyplexes that are not spherical (see Figure 2). As expected, significant aggregation was observed both for core polyplexes and upon addition of all pristine dextrans. The two lighter CMDs with the lowest charge density failed to yield stable polyplexes in complexation buffer, preventing us from evaluating their behavior at a physiological salt concentration. For the 20 kDa series, we observed a very clear correlation between the hydrodynamic diameter and the charge density that span throughout the series (see Supporting Information, Figure 4 for detailed aggregation kinetics). The two CMDs with the highest charge density of the 40 kDa series did not fully abrogate aggregation, as deduced from corresponding diameters increasing beyond 250 nm. All the other CMDs of the two heavier series yielded polyplexes that remained stable in PBS over the course of the experiment. To summarize, 10 CMDs were found unable to stabilize polyplexes in the presence of physiological PBS, as the resulting coated polyplexes readily aggregated within 15 min in those conditions. Interestingly, for some formulations the average hydrodynamic diameter decreased by 2–5 nm/min upon salt addition during the first 15 min (see Supporting Information, Figure 4). Those results suggested that internal rearrangements of polyplexes occurred within the first 15 min after the suspension medium was modified.

We conjecture that a molecular weight greater than 10 kDa is required for an efficient lateral stabilization of polyplexes in those conditions. Interestingly, even though we observed that all the CMDs of the 10 kDa series failed that step, CMD10–30 significantly lowered the polyplex growth trend. That result suggests that the influence of the charge density is not trivial: depending on the CMD series, increasing the charge density enhances the stabilization up to a point where too high an increase deteriorates the ability of the CMD coating to stabilize the polyplexes. Thus, we failed to find a simple predictive criterion for the design of a polyplex coating in terms of stability in physiological salt concentrations.

Adsorption of Plasma Proteins. Next, we assessed whether a CMD coating could prevent plasma-triggered opsonization of polyplexes. After a 30 min incubation of polyplexes or controls at 37 °C with 2% *v/v* human plasma and a subsequent centrifugation, proteins that were associated with the polyplex pellet were analyzed by nondenaturing SDS-PAGE. Representative gels are reported Figure 6A. We observed a trend from massive protein adsorption on polyplexes to negative-control levels of protein content for the four CMD series. Our systematic study reveals that the zeta potential is a strong predictive indicator of resistance to plasma protein adsorption on polyplexes. Indeed, our data suggest that a threshold zeta potential of about –20 mV is required to limit plasma protein adsorption caused by bPEI to less than 10% (see Figure 6B). Additionally, in the range that we focused on, the molecular weight of CMD was of no significant influence.

Erythrocytes Aggregation Assay. Further assays were conducted with biological material. Sheep erythrocytes aggregation assays were performed in order to gain insight into the feasibility of systemic delivery of our coated polyplexes.²⁷ The microscopic aggregation index (MAI) of each formulation was computed from image analysis. Results are reported in Figure 7. Comprehensive micrographs are reported in Supporting Information, Figure 5. Similarly to the adsorption of plasma proteins, a clear correlation of the MAI with the zeta potential was observed, although preventing erythrocytes aggregation seemed to be less demanding than opsonization. Formulations that yielded an MAI below 10% of the maximum that we measured were considered capable of preventing erythrocyte aggregation.

Uptake and Expression Profiles upon Coating and Targeting. We chose to perform all our cell-based assays in medium supplemented with 10% fetal calf serum (FCS), to set the pDNA concentration at 0.2 $\mu\text{g}/\text{cm}^2$ for transfection, and to wash the polyplexes from the cells at 4 hpt to better mimic *in vivo* conditions, as it had been repeatedly advised.^{2,10,43} Upon medium replacement at 4 hpt, we added fresh complete medium supplemented with free bPEI at a virtual N/P ratio of 24:1 in each well. That amount of polycation was found to significantly rescue polyplexes from endolysosomal entrapment without causing prohibitive cytotoxicity (data not shown), similarly to previous works.³⁹ We resorted to that measure in order to compensate for the poor endosomal escape that had been previously associated both with polyplexes at low N/P ratios such as 6:1^{39,44} and with dextran-containing nano-carriers.⁴⁵

As illustrated on Figure 8, coated polyplexes could attach to and enter cells very efficiently, up to the same performances of core polyplexes. The natural proclivity of dextran for endocytosis¹⁹ arguably explains the overall very efficient uptake of coated polyplexes by A549 cells. Reporter gene expression

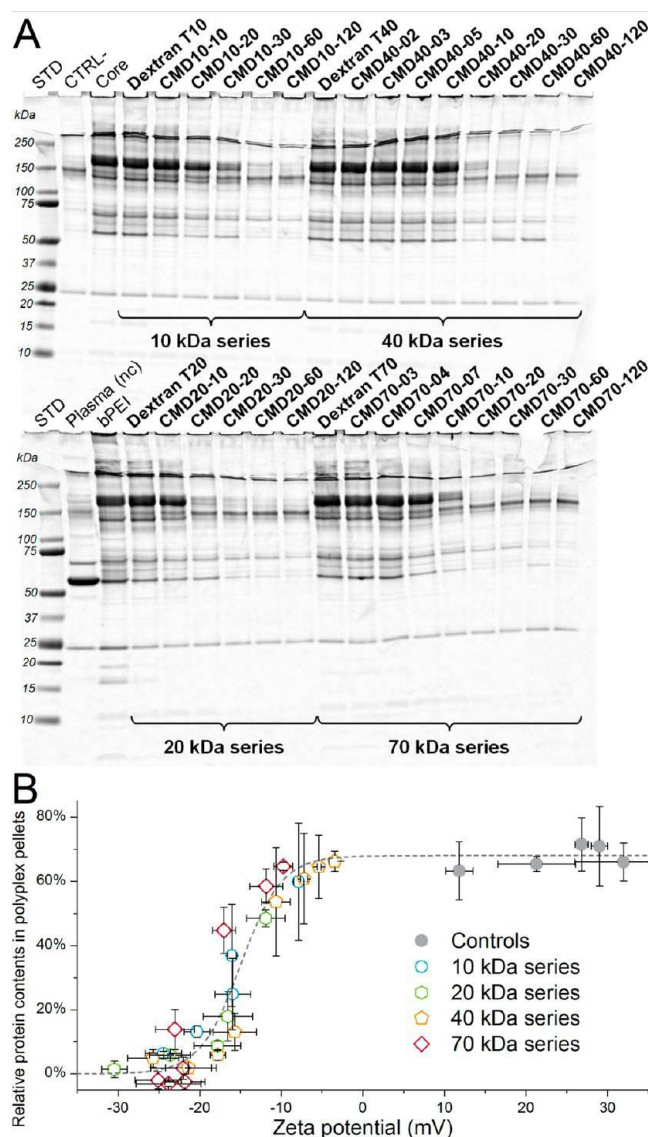


Figure 6. Impact of CMD coating upon opsonization from plasma proteins (A) and its correlation with zeta potential (B). Polyplexes were incubated with 2% *v/v* plasma from human. Samples were then centrifuged and the pellet was carefully washed and then further dissociated in nonreductive Laemmli sample buffer at 70 °C for 10 min. As a noncentrifuged (nc) control, ca. 5 μg of plasma were also analyzed (plasma (nc), bottom gel). Controls that were centrifuged with the samples include 2% *v/v* plasma from human alone (CTRL-, top gel); with core polyplexes (Core, top gel); and with bPEI at a concentration equal to the other bPEI-containing samples (bPEI, bottom gel). The relative protein content of pellets was plotted against the zeta potential of corresponding polyplexes measured in complexation buffer without plasma. The total protein material that was adsorbed onto sample tubes (CTRL-, top gel) was subtracted from the data, which were then normalized to the content of the bPEI-only control (bPEI, bottom gel). The dashed line is a guide to the eye that was centered at –15 mV. Error bars represent the standard deviations from two independent replicates.

corresponding to core polyplexes was detectable, yet very low. That result is in line with previous observations made by Ehrhardt et al.⁴⁶ In their study, they optimized transfection by 25 kDa branched PEI in the presence of 10% serum for 8 different cell lines, including A549 which they unexpectedly failed to transfect. Using such a setup provided us with a wide

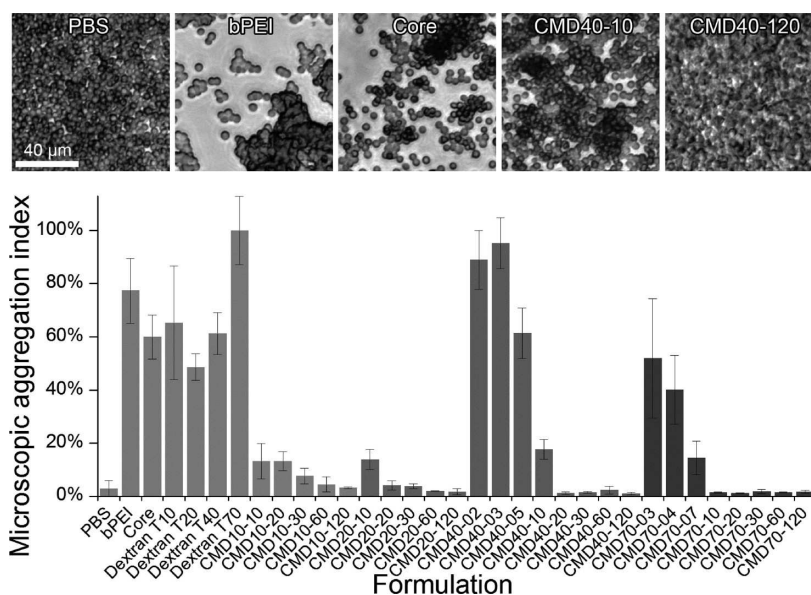


Figure 7. Erythrocyte aggregation assay. Microscopic aggregation index (MAI) relative to the Dextran T70 formulation. Error bars represent the standard deviation of MAI computed from 3 randomly acquired 270 μm × 360 μm images from each well. Upper 100 μm × 100 μm insets illustrate the representative aggregation behavior corresponding to selected formulations, from left to right: PBS, bPEI, Core, CMD40-10, and CMD40-120. Error bars represent the standard deviations from two independent replicates.

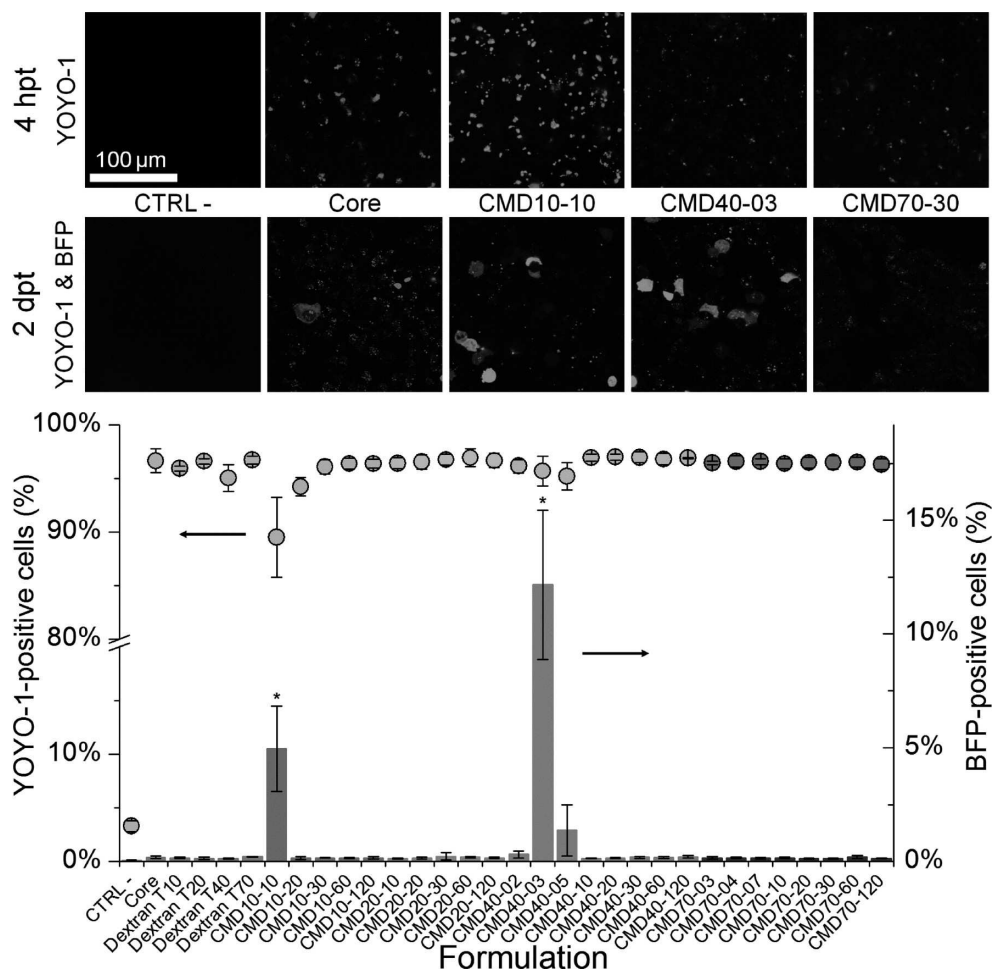


Figure 8. Transfection performances of coated polyplexes on A549 cells. Polyplexes were formed with YOYO-1-stained pDNA coding for BFP. Cytometry measurements were performed at 2 dpt: YOYO-1-positive cells (circles, left axis); BFP-positive cells (columns, right axis). Upper 200 μm × 200 μm insets illustrate selected formulations, from left to right: CTRL- (free YOYO-1-stained pDNA coding for BFP), Core, CMD10-10, CMD40-03, and CMD70-30.

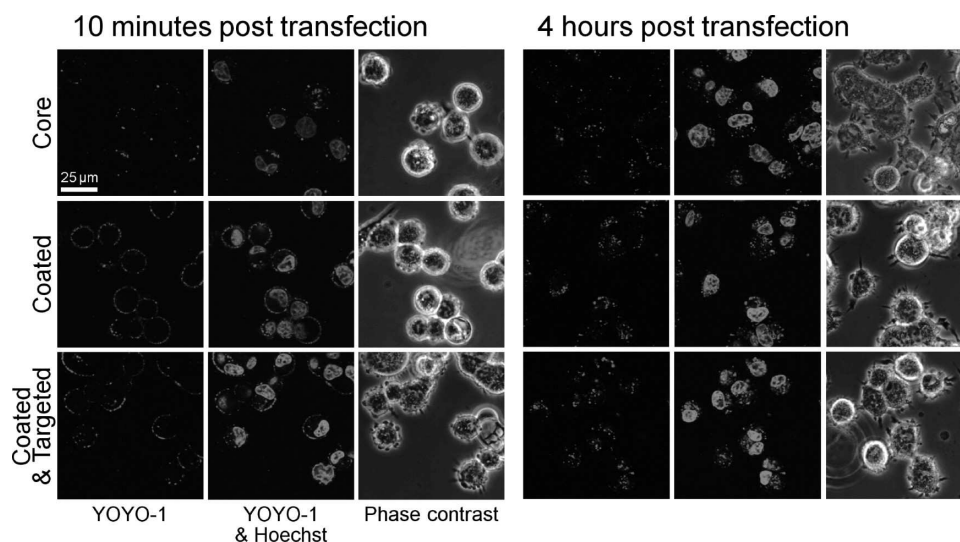


Figure 9. Illustration of polyplex binding to A549 with live confocal microscopy. Three formulations were monitored: Core polyplexes (top line), polyplexes coated with CMD70–30 (middle line), polyplexes coated with CMD70–30-Kcoil and further decorated with Ecoil-EGF at a Kcoil/Ecoil molar ratio of 1:1 and a final Ecoil-EGF concentration of 17 nM (bottom line).

Table 2. Multicriteria Evaluation of Our CMD Library for the Coating of bPEI/pDNA Polyplexes

	No coating	CMD10-10	CMD10-20	CMD10-30	CMD10-60	CMD10-120	CMD20-10	CMD20-20	CMD20-30	CMD20-60	CMD20-120	CMD40-02	CMD40-03	CMD40-05	CMD40-10	CMD40-20	CMD40-30	CMD40-60	CMD40-120	CMD70-03	CMD70-04	CMD70-07	CMD70-10	CMD70-20	CMD70-30	CMD70-60	CMD70-120
Molecular weight ^a	█	█	█	█	█	█	█	█	█	█	█	█	█	█	█	█	█	█	█	█	█	█	█	█	█	█	█
Charge density ^b	█	█	█	█	█	█	█	█	█	█	█	█	█	█	█	█	█	█	█	█	█	█	█	█	█	█	█
Encapsulation of pDNA ^c	✓	✓	✓	✓	✓	✓	✓	✓	✓	✓	✓	✓	✓	✓	✓	✓	✓	✓	✓	✓	✓	✓	✓	✓	✓	✓	✓
Protection of pDNA	✓	✓	✓	✓	✓	✓	✓	✓	✓	✓	✓	!	!	!	!	!	!	!	!	!	!	!	!	!	!	!	!
Stability in salt	×	×	×	!	×	×	✓	!	!	×	×	✓	✓	✓	✓	✓	✓	!	!	!	!	!	!	!	!	!	!
Resistance to plasma	×	×	×	!	×	×	✓	✓	✓	✓	✓	×	×	×	!	!	!	!	!	!	!	!	!	!	!	!	!
No RBC aggregation	×	!	!	✓	✓	✓	!	!	!	!	!	×	×	×	!	!	!	!	!	!	!	!	!	!	!	!	!
Attachment/uptake in A549	✓	✓	✓	✓	✓	✓	✓	✓	✓	✓	✓	!	!	!	!	!	!	!	!	!	!	!	!	!	!	!	!
Higher expression in A549	!	✓	!	!	!	!	!	!	!	!	!	!	!	!	!	!	!	!	!	!	!	!	!	!	!	!	!

^aActual figures are reported in Table 1. ^bActual figures are reported in Table 1. ^cEach CMD is considered either to validate the criterion (check), to fail the latter (cross), or to have a moderate impact on it (exclamation mark).

dynamic range to probe our CMD library for an increase in transient gene expression.

The results corresponding to the entire CMD library (Figure 8) indicate that the zeta potential that we measured in our complexation buffer is neither predictive of cellular attachment/uptake nor is it for reporter gene expression. Rather, two other characteristics of polyplexes were found to impact slightly on cellular uptake and strongly on reporter gene expression. First, the strong aggregation of polyplexes coated with CMD10–10 that was observed in complexation buffer caused the suspension to flocculate into micrometric particles. Those aggregates settled much quicker than nanoparticles in culture medium, forcing interactions with the adherent cells at the bottom of the wells. That mechanism, which is clearly irrelevant to systemic delivery, had already been pointed out as a bias of *in vitro* transfection assays.^{38,43} Second, the entrapment tightness of pDNA within polyplexes, as probed by challenging our formulations with DNase I (Figure 4), turned out to be a critical feature that increased reporter gene expression from the very low ~0.2% of core polyplexes up to ~12% upon coating with CMD40–03. Almalik et al. also recently observed a similar correlation for their chitosan-based nanocarrier coated with a

360 kDa hyaluronic acid, which has a charge density of 2.6 Θ /kDa.⁴⁷ Taken together, those observations warrant further optimization of the inner cohesion of our polyplexes in synergy with the appropriate electrostatic coating formulations that emerged from our works.

Finally, we equipped one coated polyplex formulation with a coiled-coil tethering system to demonstrate the ease of CMD biofunctionalization. This system was based on the Kcoil/Ecoil heterodimer, two complementary peptides designed to strongly and specifically bind to each other.⁴⁸ Kcoil peptides were covalently grafted on CMD by means of a thiol-vinylsulfone Michael addition. Recombinant Ecoil-tagged epidermal growth factor³² (Ecoil-EGF) was then docked to coated polyplexes by autoassembly in solution. Confocal microscopy performed at 10 mpt and later at 4 hpt illustrates the efficient binding of coated and targeted polyplexes to cells (see Figure 9, left panel). Interestingly, our coated polyplexes that were targeted to the EGFR entered cells faster than nontargeted polyplexes did, in good agreement with previously published results.³⁹ Yet, after 4 h, we observed no further differences in polyplex uptake. These results indicate that our strategy of biofunctionalization was

successful, although it did not ultimately impact on overall gene expression.

Combined results of our decoupled in vitro screening assays are summarized in Table 2, where it strikingly appears that a minimum molecular weight of 40 kDa is necessary to provide both salt stability and resistance to plasma. Indeed, for the 20 kDa series, the two only formulations that passed the former criterion were the only two that failed the latter. Four CMD formulations in the upper molecular weights and charge densities successfully validated all criteria. Unexpectedly, three unrelated formulations drastically increased the branched-PEI-based transfection of A549 cells.

CONCLUSION

We carried out a systematic analysis on a library of 26 closely related polyanions of the CMD family for the surface tailoring of a model polyplex. Results revealed marked correlations between the physicochemical properties of CMD and the behavior of corresponding nanocarriers. Overall, valuable insight was gained into the characteristics of the nanocarrier surface in relation to cargo pDNA encapsulation and protection, nanocarrier stability in salt, resistance to opsonization in human plasma, and prevention of erythrocyte aggregation: several major issues in systemic delivery.

From there, our four topmost CMD candidates thus appear highly relevant for further developments following two different strategies: on the one hand, to underlie surface biofunctionalization addressing intracellular trafficking; and on the other hand, to tailor the internal cohesion of polyplexes, a framework that is currently being developed in our laboratories.

ASSOCIATED CONTENT

Supporting Information

DLS characterization of ghost polyplexes, correlations and details in agarose gel-based assays, detailed aggregation kinetics of coated polyplexes, erythrocyte aggregation assay images, and HPLC quantification of biofunctionalized CMD. This material is available free of charge via the Internet at <http://pubs.acs.org>.

AUTHOR INFORMATION

Corresponding Author

*E-mail: gregory.decrescenzo@polymtl.ca

Notes

The authors declare no competing financial interest. The use of PEI for transfection may be covered by existing intellectual property rights, including U.S. Patent 6,013,240, European Patent 0,770,140, and foreign equivalents for which further information may be obtained by contacting licensing@polyplus-transfection.com. This is NRC publication #53291.

ACKNOWLEDGMENTS

This work was supported by the Fonds de recherche du Québec – Nature et technologies (C.F.), the Canada Research Chair on Protein-enhanced Biomaterials, and the Natural Sciences and Engineering Research Council of Canada (G.D.C.). We would like to thank B. Liberelle for setting up the carboxymethylation protocols, S. Bilodeau for NMR measurements, L. Bisson for carrying out HPLC, M. Nelea for performing SEM imaging, and S. Noël for her insightful comments.

REFERENCES

- (1) Yin, H.; Kanasty, R. L.; Eltoukhy, A. A.; Vegas, A. J.; Dorkin, J. R.; Anderson, D. G. Non-viral vectors for gene-based therapy. *Nat. Rev. Genet.* **2014**, *15* (8), 541–555.
- (2) Yousefi, A.; Storm, G.; Schifferers, R.; Mastrobattista, E. Trends in polymeric delivery of nucleic acids to tumors. *J. Controlled Release* **2013**, *170* (2), 209–218.
- (3) Laga, R.; Carlisle, R.; Tangney, M.; Ulbrich, K.; Seymour, L. W. Polymer coatings for delivery of nucleic acid therapeutics. *J. Controlled Release* **2012**, *161* (2), 537–553.
- (4) Fortier, C.; Durocher, Y.; De Crescenzo, G. Surface modification of non-viral nanocarriers for enhanced gene delivery. *Nanomedicine (London U. K.)* **2014**, *9* (1), 135–151.
- (5) Thibault, M.; Nimesh, S.; Lavertu, M.; Buschmann, M. D. Intracellular trafficking and decondensation kinetics of chitosan-pDNA polyplexes. *Mol. Ther.* **2010**, *18* (10), 1787–95.
- (6) Trubetskoy, V. S.; Wong, S. C.; Subbotin, V.; Budker, V. G.; Loomis, A.; Hagstrom, J. E.; Wolff, J. A. Recharging cationic DNA complexes with highly charged polyanions for in vitro and in vivo gene delivery. *Gene Ther.* **2003**, *10* (3), 261–71.
- (7) Hornof, M.; de la Fuente, M.; Hallikainen, M.; Tammi, R. H.; Urtti, A. Low molecular weight hyaluronan shielding of DNA/PEI polyplexes facilitates CD44 receptor mediated uptake in human corneal epithelial cells. *J. Gene Med.* **2008**, *10* (1), 70–80.
- (8) Mizrahy, S.; Raz, S. R.; Hasgaard, M.; Liu, H.; Soffer-Tsur, N.; Cohen, K.; Dvash, R.; Landsman-Milo, D.; Bremer, M. G. E. G.; Moghimi, S. M.; Peer, D. Hyaluronan-coated nanoparticles: The influence of the molecular weight on CD44-hyaluronan interactions and on the immune response. *J. Controlled Release* **2011**, *156* (2), 231–238.
- (9) Martens, T. F.; Remaut, K.; Deschout, H.; Engbersen, J. F. J.; Hennink, W. E.; van Steenberghe, M. J.; Demeester, J.; De Smedt, S. C.; Braeckmans, K. Coating nanocarriers with hyaluronic acid facilitates intravitreal drug delivery for retinal gene therapy. *J. Controlled Release* **2015**, *202* (0), 83–92.
- (10) Whitehead, K. A.; Matthews, J.; Chang, P. p. H.; Niroui, F.; Dorkin, J. R.; Severgnini, M.; Anderson, D. G. In vitro–in vivo translation of lipid nanoparticles for hepatocellular siRNA delivery. *ACS Nano* **2012**, *6* (8), 6922–6929.
- (11) Mizrahy, S.; Peer, D. Polysaccharides as building blocks for nanotherapeutics. *Chem. Soc. Rev.* **2012**, *41* (7), 2623–2640.
- (12) Raemdonck, K.; Martens, T. F.; Braeckmans, K.; Demeester, J.; De Smedt, S. C. Polysaccharide-based nucleic acid nanoformulations. *Adv. Drug Delivery Rev.* **2013**, *65* (9), 1123–1147.
- (13) Amoozgar, Z.; Yeo, Y. Recent advances in stealth coating of nanoparticle drug delivery systems. *Wiley Interdiscip. Rev.: Nanomed. Nanobiotechnol.* **2012**, *4* (2), 219–233.
- (14) Heinze, T.; Liebert, T.; Heublein, B.; Hornig, S., Functional Polymers Based on Dextran. In *Polysaccharides II*; Klemm, D., Ed.; Springer: Berlin; Heidelberg, 2006; Vol. 205, pp 199–291.
- (15) Chang, R. L. S.; Crawford, M. P.; West, M. D. An assessment of the potential use of anionic dextrans as a plasma substitute. *J. Biomed. Eng.* **1980**, *2* (1), 41–44.
- (16) Wotschadlo, J.; Liebert, T.; Heinze, T.; Wagner, K.; Schnabelrauch, M.; Dutz, S.; Müller, R.; Steiniger, F.; Schwalbe, M.; Kroll, T. C.; Höffken, K.; Buske, N.; Clement, J. H. Magnetic nanoparticles coated with carboxymethylated polysaccharide shells—Interaction with human cells. *J. Magn. Magn. Mater.* **2009**, *321* (10), 1469–1473.
- (17) Liberelle, B.; Merzouki, A.; De Crescenzo, G. Immobilized carboxymethylated dextran coatings for enhanced ELISA. *J. Immunol. Methods* **2013**, *389* (1–2), 38–44.
- (18) Moore, A.; Weissleder, R.; Bogdanov, A., Jr. Uptake of dextran-coated monocrystalline iron oxides in tumor cells and macrophages. *J. Magn. Reson. Imaging* **1997**, *7* (6), 1140–1145.
- (19) Wilhelm, C.; Billotey, C.; Roger, J.; Pons, J. N.; Bacri, J. C.; Gazeau, F. Intracellular uptake of anionic superparamagnetic nanoparticles as a function of their surface coating. *Biomaterials* **2003**, *24* (6), 1001–1011.

- (20) Schwalbe, M.; Buske, N.; Vetterlein, M.; Höffken, K.; Pachmann, K.; Clement, J. H. The carboxymethyl dextran shell is an important modulator of magnetic nanoparticle uptake in human cells. *Z. Phys. Chem.* **2006**, *220* (1_2006), 125–131.
- (21) Jiang, D.; Salem, A. K. Optimized dextran–polyethylenimine conjugates are efficient non-viral vectors with reduced cytotoxicity when used in serum containing environments. *Int. J. Pharm. (Amsterdam, Neth.)* **2012**, *427* (1), 71–79.
- (22) Kim, J. S.; Oh, M. H.; Park, J. Y.; Park, T. G.; Nam, Y. S. Protein-resistant, reductively dissociable polyplexes for in vivo systemic delivery and tumor-targeting of siRNA. *Biomaterials* **2013**, *34* (9), 2370–2379.
- (23) Sun, Y. X.; Zhang, X. Z.; Cheng, H.; Cheng, S. X.; Zhuo, R. X. A low-toxic and efficient gene vector: carboxymethyl dextran-graft-polyethylenimine. *J. Biomed. Mater. Res., Part A* **2008**, *84* (4), 1102–1110.
- (24) Ning, S.; Huang, Q.; Sun, X.; Li, C.; Zhang, Y.; Li, J.; Liu, Y. Carboxymethyl dextran-coated liposomes: Toward a robust drug delivery platform. *Soft Matter* **2011**, *7* (19), 9394–9401.
- (25) Lungwitz, U.; Breunig, M.; Blunk, T.; Gopferich, A. Polyethylenimine-based non-viral gene delivery systems. *Eur. J. Pharm. Biopharm.* **2005**, *60* (2), 247–266.
- (26) Wightman, L.; Kircheis, R.; Rossler, V.; Carotta, S.; Ruzicka, R.; Kursa, M.; Wagner, E. Different behavior of branched and linear polyethylenimine for gene delivery in vitro and in vivo. *J. Gene Med.* **2001**, *3* (4), 362–372.
- (27) Boeckle, S.; von Gersdorff, K.; van der Piepen, S.; Culmsee, C.; Wagner, E.; Ogris, M. Purification of polyethylenimine polyplexes highlights the role of free polycations in gene transfer. *J. Gene Med.* **2004**, *6* (10), 1102–1111.
- (28) Schaffert, D.; Kiss, M.; Rodl, W.; Shir, A.; Levitzki, A.; Ogris, M.; Wagner, E. Poly(I:C)-mediated tumor growth suppression in EGF-receptor overexpressing tumors using EGF-polyethylene glycol-linear polyethylenimine as carrier. *Pharm. Res.* **2011**, *28* (4), 731–741.
- (29) Grayson, A. C.; Doody, A. M.; Putnam, D. Biophysical and structural characterization of polyethylenimine-mediated siRNA delivery in vitro. *Pharm. Res.* **2006**, *23* (8), 1868–1876.
- (30) Kickhoefer, V. A.; Han, M.; Raval-Fernandes, S.; Poderycki, M. J.; Moniz, R. J.; Vaccari, D.; Silvestry, M.; Stewart, P. L.; Kelly, K. A.; Rome, L. H. Targeting vault nanoparticles to specific cell surface receptors. *ACS Nano* **2008**, *3* (1), 27–36.
- (31) Kim, I.-Y.; Kang, Y.-S.; Lee, D. S.; Park, H.-J.; Choi, E.-K.; Oh, Y.-K.; Son, H.-J.; Kim, J.-S. Antitumor activity of EGFR targeted pH-sensitive immunoliposomes encapsulating gemcitabine in A549 xenograft nude mice. *J. Controlled Release* **2009**, *140* (1), 55–60.
- (32) Boucher, C.; St-Laurent, G.; Loignon, M.; Jolicœur, M.; De Crescenzo, G.; Durocher, Y. The bioactivity and receptor affinity of recombinant tagged EGF designed for tissue engineering applications is defined by the nature and position of the tags. *Tissue Eng.* **2008**, *14* (12), 2069–2077.
- (33) Yu, Y.; Chau, Y. One-step “click” method for generating vinyl sulfone groups on hydroxyl-containing water-soluble polymers. *Biomacromolecules* **2012**, *13* (3), 937–942.
- (34) De Crescenzo, G.; Litowski, J. R.; Hodges, R. S.; O’Connor-McCourt, M. D. Real-time monitoring of the interactions of two-stranded de novo designed coiled-coils: Effect of chain length on the kinetic and thermodynamic constants of binding. *Biochemistry* **2003**, *42*, 1754–63.
- (35) Durocher, Y.; Perret, S.; Kamen, A. High-level and high-throughput recombinant protein production by transient transfection of suspension-growing human 293-EBNA1 cells. *Nucleic Acids Res.* **2002**, *30* (2), E9.
- (36) Sawant, R. R.; Sriraman, S. K.; Navarro, G.; Biswas, S.; Dalvi, R. A.; Torchilin, V. P. Polyethyleneimine-lipid conjugate-based pH-sensitive micellar carrier for gene delivery. *Biomaterials* **2012**, *33* (15), 3942–3951.
- (37) Krentsel, L.; Chaubet, F.; Rebrov, A.; Champion, J.; Ermakov, I.; Bittoun, P.; Fermandjian, S.; Litmanovich, A.; Platé, N.; Jozefonvicz, J. Anticoagulant activity of functionalized dextrans. Structure analyses of carboxymethylated dextran and first Monte Carlo simulations. *Carbohydr. Polym.* **1997**, *33* (1), 63–71.
- (38) Ogris, M.; Steinlein, P.; Kursa, M.; Mechtler, K.; Kircheis, R.; Wagner, E. The size of DNA/transferrin-PEI complexes is an important factor for gene expression in cultured cells. *Gene Ther.* **1998**, *5* (10), 1425–33.
- (39) Fortier, C.; De Crescenzo, G.; Durocher, Y. A versatile coiled-coil tethering system for the oriented display of ligands on nanocarriers for targeted gene delivery. *Biomaterials* **2013**, *34* (4), 1344–1353.
- (40) Niebel, Y.; Buschmann, M. D.; Lavertu, M.; De Crescenzo, G. Combined analysis of polycation/ODN polyplexes by analytical ultracentrifugation and dynamic light scattering reveals their size, refractive index increment, stoichiometry, porosity, and molecular weight. *Biomacromolecules* **2014**, *15* (3), 940–947.
- (41) Miyajima, T.; Yoshida, K.; Högföldt, E. Polyelectrolyte titrations. The system $\text{Na}^+ - \text{H}^+$ on carboxymethyl dextran. *J. Colloid Interface Sci.* **1993**, *156* (2), 383–387.
- (42) Buschmann, M. D.; Merzouki, A.; Lavertu, M.; Thibault, M.; Jean, M.; Darras, V. Chitosans for delivery of nucleic acids. *Adv. Drug Delivery Rev.* **2013**, *65* (9), 1234–1270.
- (43) van Gaal, E. V. B.; van Eijk, R.; Oosting, R. S.; Kok, R. J.; Hennink, W. E.; Crommelin, D. J. A.; Mastrobattista, E. How to screen non-viral gene delivery systems in vitro? *J. Controlled Release* **2011**, *154* (3), 218–232.
- (44) Thibault, M.; Astolfi, M.; Tran-Khanh, N.; Lavertu, M.; Darras, V.; Merzouki, A.; Buschmann, M. D. Excess polycation mediates efficient chitosan-based gene transfer by promoting lysosomal release of the polyplexes. *Biomaterials* **2011**, *32* (20), 4639–46.
- (45) Raemdonck, K.; Naeye, B.; Buyens, K.; Vandebroucke, R. E.; Høgset, A.; Demeester, J.; De Smedt, S. C. Biodegradable dextran nanogels for RNA interference: focusing on endosomal escape and intracellular siRNA delivery. *Adv. Funct. Mater.* **2009**, *19* (9), 1406–1415.
- (46) Ehrhardt, C.; Schmolke, M.; Matzke, A.; Knoblauch, A.; Will, C.; Wixler, V.; Ludwig, S. Polyethylenimine, a cost-effective transfection reagent. *Signal Transduction* **2006**, *6* (3), 179–184.
- (47) Almalik, A.; Day, P. J.; Tirelli, N. HA-coated chitosan nanoparticles for CD44-mediated nucleic acid delivery. *Macromol. Biosci.* **2013**, *13* (12), 1671–1680.
- (48) Triplet, B.; Yu, L.; Bautista, D. L.; Wong, W. Y.; Irvin, R. T.; Hodges, R. S. Engineering a de novo-designed coiled-coil heterodimerization domain for the rapid detection, purification and characterization of recombinantly expressed peptides and proteins. *Protein Eng.* **1996**, *9* (11), 1029–42.